Theory of phonon-drag thermopower of extrinsic semiconducting single-wall carbon nanotubes and comparison with previous experimental data

M. Tsaousidou*
Materials Science Department, University of Patras, Patras 26 504, Greece
(Received 14 December 2009; revised manuscript received 7 May 2010; published 18 June 2010)

A theoretical model for the calculation of the phonon-drag thermopower, S^g, in degenerately doped semiconducting single-wall carbon nanotubes (SWCNTs) is proposed. Detailed calculations of S^g are performed as a function of temperature, tube radius, and position of the Fermi level. We derive a simple analytical expression for S^g that can be utilized to determine the free carrier density in doped nanotubes. At low temperatures S^g shows an activated behavior characteristic of the one-dimensional character of carriers. Screening effects are taken into account and it is found that they dramatically reduce the magnitude of S^g. Our results are compared with previous published experimental data in bulk *p*-doped SWCNT materials. Excellent agreement is obtained in the temperature range 10–200 K for a consistent set of parameters. This is a striking result in view of the complexity of these systems.

DOI: 10.1103/PhysRevB.81.235425 PACS number(s): 72.20.Pa, 73.63.Fg, 63.20.kd, 63.22.Gh

I. INTRODUCTION

Thermopower, S, is an important transport coefficient that offers valuable information about the electronic structure, the scattering processes, and the mechanisms of carrier-phonon coupling in a system. In the last few years there has been growing experimental interest in S of single-wall carbon nanotubes (SWCNTs). Several groups have reported thermopower measurements on bulk SWCNT materials (e.g., mats, fibers, and films) (Refs. 1–9) and on individual SWCNTs.[10–12] However, only modest progress has been made up to now in understanding the unique features of S in these systems. Interesting issues concerning the large positive thermopower ($\sim 80\ \mu$V/K) in pristine samples,[2,4–6,8] the change in sign of S upon exposure to oxygen,[4,6] and the effect of carrier-phonon coupling[7–9,13–15] on S still remain open.

S consists of two additive contributions which are diffusion, S^d, and phonon-drag, S^g. S^d is due to the carrier diffusion in the presence of a temperature gradient and for degenerate systems varies linearly with T according to Mott's expression. S^g originates from the interchange of momentum between acoustic phonons and carriers via the carrier-phonon interaction. The first theoretical models for the study of the phonon drag in metals[16] and semiconductors[17] were developed half a century ago. More recently, extensive theoretical and experimental work has been carried out on S^g of low-dimensional semiconductor structures.[18–20]

Recent experiments on S in *p*-doped SWCNT films and fibers[8,9] provided clear evidence for the presence of S^g at $T > 15-20$ K. On the theory level, however, there is still an ongoing discussion about the role of S^g in measured thermopower.[14,15] So far, the theoretical studies of S^g are confined to metallic armchair (10,10) tubes.[8,13] However, in perfect metallic tubes with mirror electron-hole symmetry both S^d (Ref. 7) and S^g (Refs. 14 and 15) are expected to be negligibly small compared to the experimental data, due to the competition between the opposite contributions of electrons and holes. We note that the accuracy of the existing theoretical models[8,13] for S^g in metallic tubes has been questioned recently by Mahan.[15] Also, a recent theoretical work[21] pointed out that thermopower vanishes in one-dimensional (1D) conductors with a linear energy dispersion (as in the case of metallic tubes) due to electron-hole symmetry.

In this paper we propose a theoretical model for the phonon-drag thermopower in semiconducting SWCNTs that are characterized by a nonlinear energy dispersion. (A brief discussion on the behavior of S^g in this kind of nanotubes appears in Ref. 20.) We suggest that the measured thermopower in doped samples is due to the contribution of degenerate semiconducting nanotubes. In our model, S^g originates from carrier-phonon intraband scattering within the first 1D subband. As we discuss below, the dominant contribution to S^g is made by long-wavelength acoustic phonons that backscatter carriers across the Fermi surface. In this case the carrier-phonon coupling is much weaker in metallic tubes than in semiconducting tubes[22] and, consequently, S^g is expected to be substantially larger in the latter ones.

We note that upon chemical or electrostatic doping the Fermi level can be pushed into the conduction or valence band and the degenerate semiconducting tubes can be considered as one-dimensional metals. Therefore the terms "metallic" and "semiconducting" refer only to the different electronic structure in the two types of tubes (see, for example, Ref. 23).

There are two equivalent theoretical approaches to the problem of phonon drag.[20] In the first approach phonons are perturbed in the presence of a weak temperature gradient ∇T. Nonequilibrium phonons transfer part of their momentum to carriers due to the carrier-phonon coupling. Then the phonon-drag contribution to the thermoelectric current $J^g = L^g \nabla T$ is calculated by solving the coupled Boltzmann equations for carriers and acoustic phonons.[13,16,24,25] The phonon-drag thermopower is readily obtained by $S^g = -L^g/\sigma$, where σ is the carrier conductivity. In the second approach carriers are accelerated isothermally in the presence of a weak electric field $\mathbf{E}$ and impart some of their momentum to phonons due to the carrier-phonon coupling. Then the resulting phonon heat current and the phonon-drag contribution to the Peltier coefficient is calculated.[17,26–31]

This method of evaluating S^g is referred as Π approach[17] because it provides a direct estimation of the Peltier coefficient. The equivalence of the above two approaches is secured by Onsager's symmetry relation. In this paper we follow the second approach which is more general and it can be applied even in systems where carriers do not behave semiclassically.[28–31]

The paper is organized as follows. In Sec. II we introduce the theoretical model for the calculation of S^g in the semiclassical transport regime. An explicit expression for S^g is derived in Sec. II B and in Sec. II C we derive a simple approximate expression for S^g for the case of a highly degenerate semiconducting tube. Numerical results for S^g as a function of temperature, tube radius, and position of Fermi level are presented in Sec. III. In the same section we discuss the effect of screening. In Sec. IV we compare our theory with available experimental data for acid-doped bulk SWCNT samples.

II. THEORY

A. Description of the physical system

We assume that the nanotube is a long indefinitely thin cylinder of radius R and length L. The nanotube axis is along the z direction. The carrier wave function is[32]

$$\Psi_{lk}(\mathbf{r}) = \frac{1}{\sqrt{L}} e^{ikz} \frac{1}{\sqrt{2\pi}} e^{il\theta} \frac{1}{\sqrt{R}} \delta(r - R), \tag{1}$$

where, $\mathbf{r}$ is the space vector, k is the carrier wave vector along the axial direction, θ is the azimuthal angle, and l labels 1D orbital subbands associated with the carrier confinement along the circumference. We assume that the Fermi level, E_F, is located between the first and the second 1D subbands (i.e., only the ground subband is occupied). Then, the carrier energy is

$$E_k = E_1 + \frac{\hbar^2 k^2}{2m^*}, \tag{2}$$

where m^* is the carrier effective mass and E_1 denotes the position of the first van Hove singularity.

In carbon nanotubes phonons also exhibit 1D character. The lattice displacement at a point $\mathbf{r}$ is[22]

$$\mathbf{u}(\mathbf{r}) = \hat{\eta}_{mq} e^{iqz} e^{im\theta}, \tag{3}$$

where, $\hat{\eta}_{mq}$ is the polarization vector, q is the phonon wave vector in the axial direction and $m=0, \pm 1, \pm 2, \ldots$ denotes the phonon modes associated with phonon confinement along the circumference. Due to the conservation of angular momentum only the three low-energy acoustic modes with $m=0$ (the so-called twisting, stretching, and breathing modes) contribute to the carrier-phonon intraband scattering. The phonon frequencies and polarization vectors have been calculated within the continuum model proposed by Suzuura and Ando.[22]

The carrier-phonon interaction in carbon nanotubes has been studied in several texts within the tight-binding approximation[33–37] or a continuous elastic theory.[22,38–40] Here we follow the continuous model of Suzuura and Ando[22] according to which the carrier-phonon coupling is described via the acoustic deformation potential,

$$U(\mathbf{r}) = D\left(\frac{1}{R}\frac{\partial u_\theta}{\partial \theta} + \frac{\partial u_z}{\partial z} + \frac{u_r}{R}\right), \tag{4}$$

where D is the deformation-potential constant. The deformation-potential approximation provides a good description of the carrier interaction with long-wavelength acoustic phonons. The last term in Eq. (4) accounts for the nonzero curvature of the nanotube.[22] The twisting mode does not participate to carrier-phonon scattering via the deformation-potential coupling. Moreover, in the long-wavelength limit ($qR \ll 1$), which is the regime of our interest, the breathing mode is dispersionless and does not contribute to S^g. Thus, in what follows we consider only the stretching mode which is characterized by a linear dispersion $\omega_q = v_s|q|$, where v_s is the sound velocity. The phonon polarization vector, $\hat{\eta} = (\eta_\theta, \eta_z, \eta_r)$, for this mode in the limit $qR \ll 1$ is

$$\hat{\eta}_q = \left(0, \frac{1}{a}, \frac{-i\nu qR}{a}\right), \tag{5}$$

where $a = \sqrt{1 + \nu^2 q^2 R^2}$ and ν is Poisson's ratio. Ignoring the terms proportional to q^2R^2 the above expression becomes identical with the one derived by De Martino *et al.*[41]

B. An explicit expression for the phonon-drag thermopower

We assume a small electric field E in the axial direction of the nanotube. The presence of E creates a net flux of carriers along the axis of the tube which results in a momentum transfer to phonons through the carrier-phonon coupling. We calculate the resulting phonon heat flux Q and obtain the phonon-drag contribution to the transport coefficient,

$$M^g = Q/E. \tag{6}$$

To get S^g we utilize the Onsager's relation

$$S^g = \frac{M^g}{T\sigma}, \tag{7}$$

where σ is the carrier conductivity and T the absolute temperature.

The phonon heat flux is given by

$$Q = \frac{1}{L}\sum_q \hbar \omega_q v_q N_q^1, \tag{8}$$

where $v_q = v_s q/|q|$ is the phonon group velocity and $N_q^1 = N_q - N_q^0$ is the first-order perturbation of the phonon distribution function.

The perturbation N_q^1 is determined by the steady-state Boltzmann equation for phonons in the relaxation-time approximation when $\nabla T = 0$. Namely,

$$-\frac{N_q^1}{\tau_{ph}} + \left(\frac{\partial N_q}{\partial t}\right)_{ph\text{-}c} = 0, \tag{9}$$

where τ_{ph} is the phonon relaxation time associated with phonon-phonon collisions and phonon scattering by imper-

fections. For simplicity we have ignored the dependence of τ_{ph} on q. $(\partial N_q/\partial t)_{ph\text{-}c}$ is the rate of change in the phonon distribution function N_q due to phonon scattering by carriers. It is written in the standard form,

$$\left(\frac{\partial N_q}{\partial t}\right)_{ph\text{-}c} = g_s g_v \sum_{k,k'} f_{k'}(1-f_k)P_q^e(k',k) - f_k(1-f_{k'})P_q^a(k,k'), \tag{10}$$

where g_s and g_v are the spin and the valley degeneracies, respectively, f_k is the carrier distribution function, and $P_q^{a(e)}(k,k')$ are the transition rates at which the carrier in a state k is promoted to a state k' by absorbing (emitting) one phonon with wave vector q.

When the external field E is weak, Eq. (10) is linearized and is solved in terms of N_q^1. Then we get

$$\left(\frac{\partial N_q}{\partial t}\right)_{ph\text{-}c} = -\frac{N_q^1}{\tau_{pc}(q)} + \frac{g_s g_v}{k_B T}\sum_{k,k'} \Gamma_{k',k} \times \left(\frac{f_k^1}{df_k^0/dE_k} - \frac{f_{k'}^1}{df_{k'}^0/dE_{k'}}\right), \tag{11}$$

where $\tau_{pc}(q)$ is the phonon relaxation time associated with scattering by carriers given by

$$\tau_{pc}^{-1}(q) = g_s g_v \sum_{k,k'} \Gamma_{k',k}/[N_q^0(N_q^0+1)] \tag{12}$$

and $\Gamma_{k',k}$ is the average equilibrium rate of absorption of phonons with wave vector q. It is given by

$$\Gamma_{k',k} = f_k^0(1-f_{k'}^0)P_q^{a0}(k,k'), \tag{13}$$

where $f_k^0 \equiv f^0(E_k) = \{\exp[\beta(E_k - E_F)]+1\}^{-1}$ (with $\beta = 1/k_B T$) is the Fermi-Dirac function and $P_q^{a0}(k,k')$ denotes the transition rate in equilibrium.

Assuming that phonon-phonon scattering and phonon scattering by impurities dominate over the phonon-carrier scattering ($\tau_{pc} \gg \tau_{ph}$), Eqs. (9) and (11) give

$$N_q^1 = \frac{g_s g_v \tau_{ph}}{k_B T}\sum_{k,k'} \Gamma_{k',k}\left(\frac{f_k^1}{df_k^0/dE_k} - \frac{f_{k'}^1}{df_{k'}^0/dE_{k'}}\right). \tag{14}$$

In the above equation f_k^1 is the first-order perturbation of the carrier distribution function.

It is worth noting that Eq. (14) can be regarded as a starting point for the calculation of S^g in all the problems treated within the Π approach.[20] Now, by substituting the phonon perturbation into Eq. (8) we take for the heat flux,

$$Q = \frac{g_s g_v \tau_{ph}}{L k_B T}\sum_{k,k',q} \hbar\omega_q v_q \Gamma_{k',k}\left(\frac{f_k^1}{df_k^0/dE_k} - \frac{f_{k'}^1}{df_{k'}^0/dE_{k'}}\right). \tag{15}$$

To determine the perturbation of the carrier distribution function f_k^1 entering Eq. (15) we use the 1D steady-state Boltzmann equation,

$$\frac{e}{\hbar}E\frac{\partial f_k}{\partial k} = \left(\frac{\partial f_k}{\partial t}\right)_{coll}, \tag{16}$$

where e is the carrier charge and the right-hand side of Eq. (16) is the rate of change in the carrier distribution function due to elastic collisions with static imperfections. In the relaxation-time approximation this term is written as $-f_k^1/\tau(E_k)$, where $\tau(E_k)$ is the carrier relaxation time. Equation (16) is linearized to give

$$f_k^1 = -eE\tau(E_k)v_k\left(\frac{df_k^0}{dE_k}\right), \tag{17}$$

where $v_k = (1/\hbar)\nabla_{\mathbf{k}}E_k = \hbar k/m^*$ is the carrier group velocity.

By substituting Eq. (17) into Eq. (15) and making use of Eqs. (6), (7), and (13) we finally get

$$S^g = -\frac{g_s g_v e\tau_{ph}}{\sigma L k_B T^2}\sum_{k,k',q} \hbar\omega_q v_q[\tau(E_k)v_k - \tau(E_{k'})v_{k'}] \times f_k^0(1-f_{k'}^0)P_q^{a0}(k,k'). \tag{18}$$

The above expression is equivalent to the expression derived by Kubakaddi and Butcher[25] for a quantum wire coupled to three-dimensional (3D) phonons. The authors in Ref. 25 followed a different approach than this described here. They followed Bailyn's theory[16] and they calculated the phonon-drag contribution to the thermoelectric current that originates from the carrier scattering with nonequilibrium phonons in the presence of a small temperature gradient across the wire. Their calculation was based on the solution of the coupled Boltzmann equations for electrons and phonons.

The transition rate $P_q^{a0}(k,k')$ is calculated by using Fermi's golden rule. The lattice displacement for the stretching mode is written in second quantized form,

$$\mathbf{u}(\mathbf{r}) = \sum_q \sqrt{\frac{\hbar}{2A\rho\omega_q}}(\hat{\eta}_q e^{iqz}\alpha_q + \hat{\eta}_q^* e^{-iqz}\alpha_q^+), \tag{19}$$

where α_q^+ and α_q are the phonon creation and annihilation operators, respectively, $A = 2\pi RL$ is the nanotube surface area and ρ is the mass density. For the stationary carrier states considered here one easily finds

$$P_q^{a0}(k,k') = \frac{2\pi}{\hbar}N_q^0\frac{|U_q|^2}{\epsilon^2(|q|,T)}\delta(E_{k'} - E_k - \hbar\omega_q)\delta_{k',k+q}, \tag{20}$$

where $N_q^0 = [\exp(\beta\hbar\omega_q)-1]^{-1}$ is the phonon distribution in equilibrium, $|U_q|^2$ is the square of the carrier-phonon matrix element for the deformation-potential coupling, and $\epsilon(|q|,T)$ is the 1D static dielectric function. By utilizing Eqs. (4), (5), and (19) the matrix elements $|U_q|^2$ in the limit $qR \ll 1$ are written as

$$|U_q|^2 = \frac{\hbar\Xi^2 q^2}{2A\rho\omega_q}, \tag{21}$$

where $\Xi = D(1-\nu)$. We note that the q dependence of $|U_q|^2$ is typical for the carrier interaction with longitudinal-acoustic phonons via an isotropic deformation potential.[42] A similar

expression to the one we derive here is given in Ref. 39.

The dielectric function for a 1D gas confined to the surface of the carbon nanotube is calculated within the random-phase approximation.[32,43] For the carrier wave functions considered here we obtain

$$\epsilon(|q|,T) = 1 + \frac{4g_v e^2 m^*}{\hbar^2 \pi \epsilon_b} \frac{1}{|q|} K_0(|q|R) I_0(|q|R) M(|q|,T), \tag{22}$$

where I_0 and K_0 are the modified Bessel functions of the first and the second kind, respectively, and ϵ_b is the background dielectric constant. $M(|q|,T)$ is the standard factor that accounts for finite-temperature effects on the static polarization function[43,44]

$$M(|q|,T) = \beta \int_{E_1}^{\infty} dE_k \frac{\ln|(q+2k)/(q-2k)|}{4\cosh^2[\beta(E_k - E_F)/2]}. \tag{23}$$

To obtain an explicit expression for S^g we substitute Eq. (20) into Eq. (18). Then the summation over k' is readily carried out by replacing k' by $k+q$ as a consequence of the momentum conservation condition imposed by the Kronecker symbol $\delta_{k',k+q}$. Moreover, the summations over q and k are transformed to the integrals

$$\sum_q \to \frac{L}{2\pi}\int_{-\infty}^{\infty} dq \quad \text{and} \quad \sum_k \to \frac{L}{2\pi}\int_{-\infty}^{\infty} dk.$$

The presence of the δ function in Eq. (20) allows the immediate evaluation of the k integration. We see by inspection that

$$\delta(E_{k+q} - E_k - \hbar\omega_q) = \frac{2m^*}{\hbar^2|q|}\delta(2k + q \mp q_0), \tag{24}$$

where $q_0 = 2v_s m^*/\hbar$. The minus and the plus signs correspond, respectively, to positive and negative q.

Now, after some algebra, we finally obtain

$$S^g = \frac{m^* \Xi^2 l_{ph}}{2\pi e \rho R k_B T^2} \int_0^{\infty} dq \frac{q}{\epsilon^2(|q|,T)} \frac{q}{2k_F} N_q^0 I(q), \tag{25}$$

where $l_{ph} = v_s \tau_{ph}$ is the phonon-mean-free path, $k_F = [2m^*(E_F - E_1)/\hbar^2]^{1/2}$ is the Fermi wave number, and $I(q)$ is the product of the Fermi occupation factors

$$I(q) = f^0(E_k)[1 - f^0(E_k + \hbar\omega_q)] \tag{26}$$

with $k = |q_0 - q|/2$. In deriving Eq. (25) we have ignored the energy dependence of the carrier relaxation time and in Eq. (18) we have replaced $\tau(E_k)$ by its value at the Fermi level, τ_F. This is a good approximation when $\hbar\omega_q \ll E_F$.[45] Moreover, we have replaced σ by $ne^2\tau_F/m^*$, where $n = g_s g_v k_F/\pi$ is the density of carriers per unit length. Interestingly, S^g becomes independent of the carrier relaxation time.

C. An approximate expression for S^g

At low T and assuming that $\hbar\omega_q$ is a small quantity compared to E_F the product $I(q)$ is approximated by[24]

$$I(q) \approx \hbar\omega_q (N_q^0 + 1)\delta(E_k - E_F) \tag{27}$$

with $k = |q_0 - q|/2$. The δ function can be written in the following form:

$$\delta(E_k - E_F) = \frac{2m^*}{\hbar^2 k_F}[\delta(q - q_0 - 2k_F) + \delta(q - q_0 + 2k_F)]. \tag{28}$$

We see that $\delta(E_k - E_F)$ resonates at $q = q_0 + 2k_F$ for positive q. When the expression (27) for $I(q)$ is substituted into Eq. (25) the integration over q is carried out straightforwardly by using the condition $q = q_0 + 2k_F$. We note that $q_0 \ll 2k_F$ and consequently, stretching phonons with $q = 2k_F$ make the dominant contribution to S^g.

Equation (25) is now significantly simplified and is written in the convenient approximate form

$$S^g = \frac{C}{T^2} \frac{1}{\epsilon^2(2k_F,T)} \frac{e^{\beta\hbar\omega_{2k_F}}}{(e^{\beta\hbar\omega_{2k_F}} - 1)^2}, \tag{29}$$

where C is given by

$$C = \frac{2(m^*)^2 \Xi^2 l_{ph} \omega_{2k_F}}{\pi\hbar e \rho R k_B}. \tag{30}$$

In the above equations, $\omega_{2k_F} = v_s 2k_F$ is the frequency of a stretching phonon with $q = 2k_F$ and $\epsilon(2k_F,T)$ is an approximate expression for the dielectric function. To obtain $\epsilon(2k_F,T)$, we replace q by $2k_F$ in the denominator and in the arguments of the modified Bessel functions I_0 and K_0 in Eq. (22). The factor $M(|q|,T)$ is replaced by the average $\bar{M}(2k_F,T)$ that is given by the expression,

$$\bar{M}^{-2}(2k_F,T) = \frac{\int_0^{\infty} dq q^2 M^{-2}(|q|,T) N_q^0 I(q)}{\int_0^{\infty} dq q^2 N_q^0 I(q)}. \tag{31}$$

$\bar{M}(2k_F,T)$ has been evaluated numerically for several values of k_F and R and we find that in the degenerate limit and when $T_F > 5\hbar\omega_{2k_F}/k_B$ [where $T_F = (E_F - E_1)/k_B$ is the Fermi temperature] the following expression provides a very good fit

$$\bar{M}(2k_F,T) = \ln\left(\frac{4k_F + q_0}{q_0}\right)[\alpha_1 - \alpha_2 \exp(-\alpha_3 x)], \tag{32}$$

where $x = \beta\hbar\omega_{2k_F}$, $\alpha_1 = 1.175 \pm 0.002$, $\alpha_2 = 0.60 \pm 0.01$, and $\alpha_3 = 0.41 \pm 0.01$. At low T the effect of screening is severe and unity can be neglected in Eq. (22). In this case, the T dependence of the dielectric function is described by Eq. (32).

At temperatures where $\beta\hbar\omega_{2k_F} \gg 1$ the dielectric function shows a weak T dependence. Then S^g follows the law,

$$S^g \propto \frac{1}{T^2} e^{-\beta\hbar\omega_{2k_F}}. \tag{33}$$

This activated behavior is characteristic in 1D systems where the Fermi surface consists of two discrete points $\pm k_F$.[46,47]

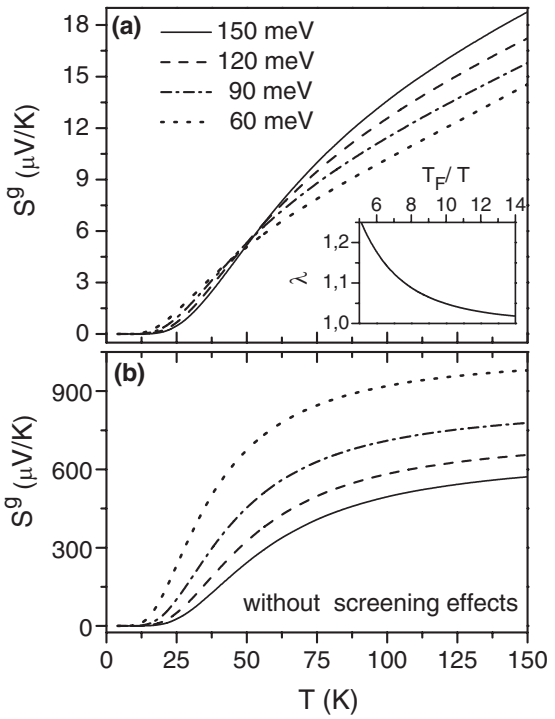

FIG. 1. S^g against temperature for a SWCNT of radius 0.5 nm. Results are shown for four values of E_F-E_1: 60 meV (dotted line), 90 meV (dashed-dotted line), 120 meV (dashed line), and 150 meV (solid line) (a) when screening is taken into account and (b) when screening is ignored. The phonon-mean-free path is taken to be 1 μm. The inset shows the ratio $\lambda=S^g/S^g_{appr}$ as a function of T_F/T.

We note that when screening is ignored and the phonon-mean-free path is constant the T dependence of S^g given by Eq. (29) is similar to what predicted by Scarola and Mahan[13] for an armchair (10,10) metallic SWCNT due to interband electron scattering between the two linear bands. However, the absolute magnitude of S^g in a metallic tube is expected to be much lower than that predicted in Ref. 13 due to the competing contributions of electrons and holes to the thermoelectric current.

III. NUMERICAL RESULTS

We assume that the free carriers are holes and we examine the dependence of S^g on temperature, the radius of the nanotube, and the position of the Fermi level with respect to the position of the first van Hove singularity. The analysis is the same for the case of electrons with the only difference being the sign of S^g. The values for the material parameters used in the calculations are $g_s=g_v=2$, $D=24$ eV,[22,48] $\nu=0.2$,[49] $\epsilon_b/4\pi\epsilon_0=2.4$,[32] $\rho=3.8\times10^{-7}$ Kgr/m^2, and $v_s=19.9$ km/s.[22] The hole effective mass is taken to be $m^*=m_e/22.7\tilde{R}$, where $\tilde{R}$ is the tube radius in nanometers.[49] We assume that $l_{ph}=1$ μm.

In Fig. 1(a), we show the S^g evaluated from Eq. (25) for a p-type SWCNT of radius 0.5 nm as a function of T. The solid, dashed, dashed-dotted, and dotted lines correspond, respectively, to $E_F-E_1=150$ meV, 120 meV, 90 meV, and 60 meV. We note that at temperatures where the carriers are nondegenerate we have taken into account the thermal broadening effects on σ. To assure the accuracy of the approximate expression (29), in the inset of Fig. 1 we show the ratio $\lambda=S^g/S^g_{appr}$ as a function of T_F/T for $E_F-E_1=60$ meV. S^g and S^g_{appr} are calculated from Eqs. (25) and (29), respectively. Calculations of λ for 90, 120, and 150 meV also fall on to the same curve. We can see that in the degenerate limit the approximate result agrees very well with the exact expression for S^g. Finally, in Fig. 1(b) S^g is calculated in the absence of screening, $\epsilon(|q|,T)=1$. It turns out that screening induces a strong suppression of S^g by 1–2 orders of magnitude. Inspection of Eq. (22) shows that screening effects become more severe as R decreases. We note that in the absence of screening S^g levels off at high T in agreement with previous estimations in metallic SWCNTs.[8,13] However, when screening is introduced S^g shows a quasilinear T dependence at high T due to the temperature dependence of the dielectric function. The dielectric function $\epsilon(2k_F,T)$ as a function of the inverse temperature for a SWCNT with $R=0.5$ nm is shown in Fig. 2

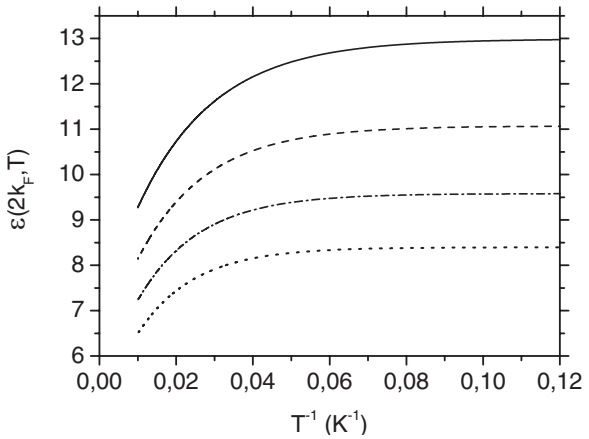

FIG. 2. Dielectric function at $q=2k_F$ as a function of the inverse temperature for a SWCNT of radius 0.5 nm. The solid, dashed, dashed-dotted, and dotted lines correspond to $k_F=0.4$ nm^{-1}, 0.45 nm^{-1}, 0.5 nm^{-1}, and 0.55 nm^{-1}, respectively.

In Fig. 3 we show the dependence of S^g on the Fermi level with respect to the position of the first van Hove sin-

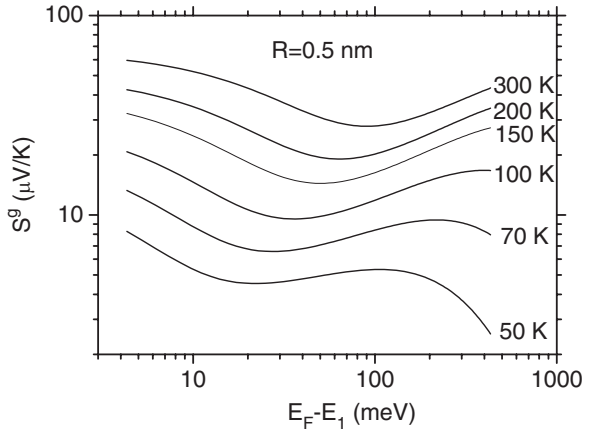

FIG. 3. S^g as a function of E_F-E_1 for various temperatures. The phonon-mean-free path is 1 μm.

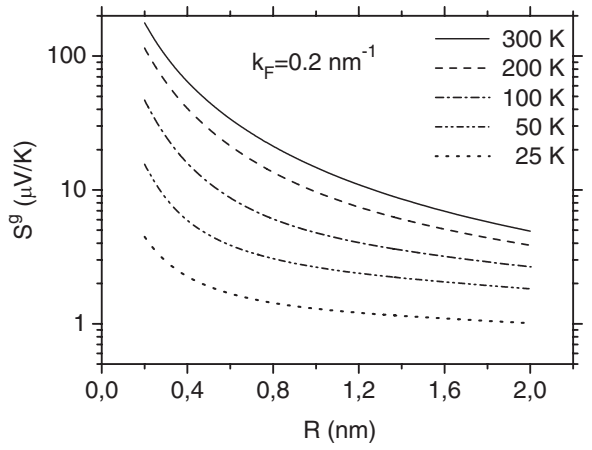

FIG. 4. S^g as a function of the nanotube radius for various temperatures. $l_{ph}=1$ μm. At $T\geq 100$ K S^g follows approximately a $R^{-1.5}$ law.

gularity for temperatures $50\leq T\leq 300$ K. The shown structure is due to two competing mechanisms, which are the suppression of the carrier-phonon scattering and the increase in $1/\epsilon(q)$ as k_F increases. The tube radius is 0.5 nm.

Finally, in Fig. 4 we present the calculated values of S^g as a function of the nanotube radius. At temperatures higher than 100 K we find that S^g follows a law close to $S^g \propto R^{-1.5}$. At lower temperatures S^g shows a weaker dependence on R especially at large values of R.

IV. COMPARISON WITH THE EXPERIMENT—DISCUSSION

So far there is no clear evidence about the phonon-drag effect in isolated SWCNTs. The most relevant experiments were performed by Yu *et al.*[11] in an individual SWCNT at temperatures above 100 K. The observed thermopower showed a linear T dependence which was attributed to the linear diffusion component and a constant phonon-drag component of about 6 μV/K without, however, excluding the possibility of an additional contact effect. According to our analysis in Sec. III, the phonon-drag thermopower at relatively high temperatures shows a quasilinear T dependence and this makes difficult the separation of the diffusion and the phonon-drag contributions. Nevertheless, when the calculated values for S^g shown in Fig. 1(a) are fitted by a linear function of T we find that the intercepts vary from 1.4 to 7.4 μV/K when the position of the Fermi level with respect to the first van Hove singularity varies from 60 to 150 meV. These values are in agreement with the experimental estimation of S^g in Ref. 11. We note that the intercepts depend linearly on the phonon-mean-free path and vary approximately as $R^{-1.5}$.

Vavro *et al.*[8] and Zhou *et al.*[9] have reported thermopower measurements in p-doped bulk SWCNT samples in a wide temperature range (10–200 K) that show clearly the signature of phonon drag. Normally, in bulk samples nanotubes are self-organized into long "ropes," which contain a large number of nanotubes (tens to hundreds),[50] forming a 3D network of complex geometry. Thermopower in these nanotube networks exhibits a very similar behavior as this of an individual nanotube described in Sec. III. We have recently proposed a simple argument based on a model of parallel conductors which suggests that in a network with homogeneous doping and with a narrow distribution of tube diameters the measured thermopower resembles that of an individual tube.[20] The resistivity measurements in the samples under consideration showed weak coupling between metallic nanotubes[9] and hence the contribution from metallic tubes to the total conductivity is neglected. We also recall that the contribution of metallic tubes in S is expected to be small compared to this of semiconducting tubes. Therefore, we can use the theory for isolate semiconducting SWCNTs developed here to interpret the data in Refs. 8 and 9.

In Fig. 5 the circles are the measured thermopower for a bulk sample prepared by pulsed laser vaporization (PLV) and doped with HNO_3.[9] The tube radius is $R=0.68\pm 0.04$ nm. At low temperatures (up to 100 K) we fit the data for the total thermopower, S, by the expression

$$S=\frac{C}{T^2}\frac{1}{\epsilon^2(2k_F,T)}\frac{e^{\beta\hbar\omega_{2k_F}}}{(e^{\beta\hbar\omega_{2k_F}}-1)^2}+AT(1-B\ln T). \quad (34)$$

The first term is the approximate expression (29) for S^g and the second term corresponds to the diffusion component S^d. The sample is highly degenerate and at temperatures up to 100 K Eq. (29) accurately describes S^g. The T dependence introduced by the dielectric function is given by Eq. (32). The values we obtained for the parameters k_F, A, and B are shown in Table I.

The logarithmic term in S^d secures an excellent fit to the measured thermopower at all temperatures up to 100 K. If this term is neglected the theoretical values for the total thermopower are significantly larger than the experimental ones at high temperatures. We speculate that the $T\ln T$ term in S^d is due to two-dimensional (2D) weak localization (WL) effects.[51] If this speculation is valid we would also expect a signature of WL in the conductivity measurements. We note that the relative change in conductivity should be the same as

TABLE I. The values for the parameters A, B, and k_F obtained from the fit of the thermopower data (Refs. 8 and 9) for $T\leq 100$ K by using Eq. (34). In the last column, we show for comparison the values for B' obtained from the resistivity data (Refs. 9 and 57) in the range 10–100 K.

	A (μV/K^2)	k_F (nm^{-1})	B	B'
PLV film+HNO_3	0.184 ± 0.003	0.40 ± 0.01	0.132 ± 0.002	0.131 ± 0.002
HiPco fiber+H_2SO_4	0.083 ± 0.007	0.57 ± 0.01	0.156 ± 0.013	0.222 ± 0.003

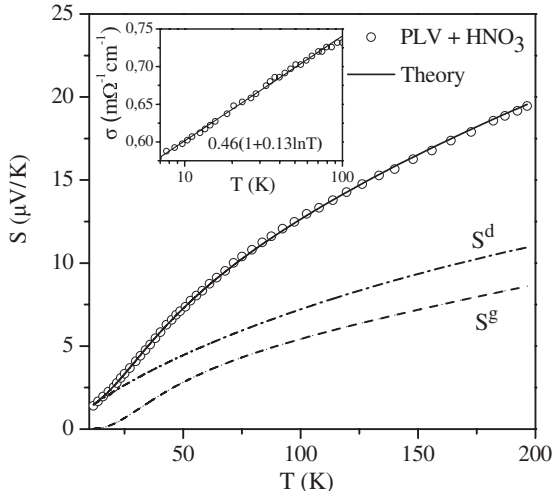

FIG. 5. Thermopower versus temperature. The circles are the experimental data for a bulk sample prepared by pulsed laser vaporization and doped with HNO_3 (Ref. 9). The solid line is the total thermopower of an individual nanotube obtained as explained in text. The dashed and the dashed-dotted lines correspond to the phonon-drag and the diffusion contributions, respectively. In the inset, the circles are the conductivity data (Ref. 9) and the solid line is the fit by using Eq. (35).

in S^d but with an opposite sign.[51,52] Interestingly, we find that at temperatures $10 \leq T \leq 100$ K the conductivity follows the law,

$$\sigma = \sigma_0(1 + B' \ln T), \tag{35}$$

where the value of B' is shown in Table I. We see that B and B' agree to each other remarkably well. The origin of the 2D WL in these samples is not well understood. It is likely related to the individual rope although in this case a 1D localization behavior would be expected.[53] However, the phase coherence length, in the samples we discuss here, is comparable to the diameter of the rope[54] and the 2D limit might be approached. Langer *et al.*[55] have also observed a ln T dependence of the conductance for an individual multiwall CNT at 0.1–100 K which was attributed to 2D WL. Finally, we should remark that WL is expected to have a negligible effect on S^g.[56]

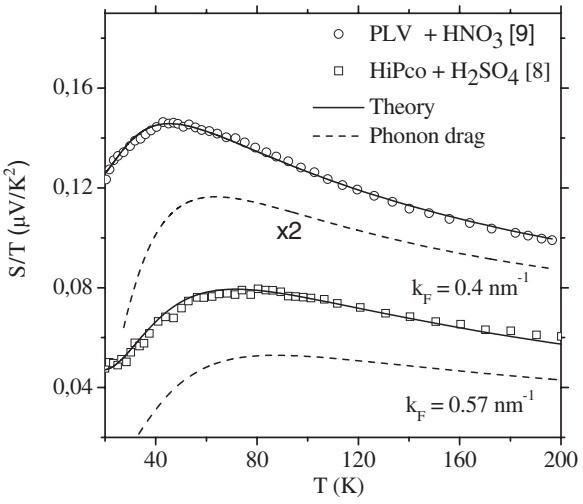

FIG. 6. The ratio S/T as a function of temperature. The symbols are the experimental data for two bulk samples (Refs. 8 and 9). The solid lines denote the total thermopower of an individual nanotube obtained as explained in text. The dashed lines are the phonon-drag contributions. For clarity the calculated S^g that corresponds to the $PLV+HNO_3$ sample has been multiplied by the factor 2. The peaks shown in the measured S/T are associated to the phonon-drag effect.

Now, by using the values for k_F we obtained from the fitting of the thermopower data at low T, we calculate S^g in the whole temperature range from 10 to 200 K by using the exact expression (25). The only remaining unknown is the value of the phonon-mean-free path l_{ph} which is determined from the experimental data when the diffusion contribution is subtracted. We find that $l_{ph}=0.6$ nm. This value is consistent with the values 0.25–0.75 μm reported recently for an individual SWCNT.[11] Our estimation for the total thermopower is shown as solid line in Fig. 5. The dashed and the dashed-dotted lines correspond to the phonon-drag and the diffusion contributions, respectively.

By following a similar procedure as described above we have interpreted the thermopower data for another bulk sample prepared by high-pressure decomposition of CO (HiPco) and doped with H_2SO_4.[8] The tube radius varied from 0.4–0.7 nm. Conductivity measurements for this sample (designated as HPR93C) appear in Ref. 57. The experimental data for the ratio S/T are shown as squares in Fig. 6. The values for the fitting parameters k_F, A, and B are shown in Table I. We also present the value of B' for comparison. In the calculations the tube radius is taken to be the average $R=0.55$ nm while for the phonon-mean-free path we obtained the value $l_{ph}=0.4$ nm. The calculated values for S/T is shown as solid line in Fig. 6.

Concerning the consistency of the fitting parameters A and k_F we should make the following remarks. By using the values for k_F shown in Table I and a simple tight-binding model for the estimation of the first van Hove singularity (see, for example, Ref. 49) the values we get for E_F are in good agreement with those determined from reflectivity and Raman measurements.[9] Also, A varies inversely with k_F^2 in agreement with Mott's expression for S^d. Moreover, the values we extract for k_F support recent arguments according to which H_2SO_4 is a stronger dopant than HNO_3.[9] Namely, according to our estimation for the Fermi wave numbers, the Fermi level is shifted by 94 meV and 155 meV below the top of the valence band for the $PLV+HNO_3$ and HiPco $+H_2SO_4$ samples, respectively.

In order to show clearly the effect of phonon drag in Fig. 6 we have plotted the ratio S/T as a function of T. The circles and the squares are the measured values for the samples $PLV+HNO_3$ and $HiPco+H_2SO_4$, respectively. The dashed lines are the theoretical estimates for S^g and the solid lines are the calculated values for the total thermopower. The peaks at $T=T^*$ are associated to phonon-drag thermopower. The shift between the experimental and the theoretical values for T^* is due to the logarithmic term in S^d. The position of the peak moves toward to higher temperatures as doping increases. This dependence can be understood by maximiz-

ing the ratio S^g/T using Eq. (29). Then we get the following dependence:

$$T^* = 1.1\frac{\hbar v_s k_F}{k_B}. \quad (36)$$

It is important to add that the exponential suppression of S^g at low temperatures is unique for 1D systems. In higher dimensions S^g exhibits a power-law T dependence at low temperatures.[19,20] The observed peak in S/T, which is ascribed to phonon drag, underlies the 1D character of thermopower. This adds another confirmation that thermopower in bulk carbon nanotube-based materials is a property of the individual tube rather than a property of the network.

V. CONCLUSIONS

In summary, we have presented a rigorous model for the calculation of the phonon-drag thermopower in degenerately doped semiconducting SWCNTs. By using the derived model we investigated the dependence of S^g on temperature, tube radius, and position of the Fermi level. We found that S^g decreases with the increase in the tube radius following approximately a $R^{-1.5}$ law at high temperatures. In the degenerate limit, we derive a simple expression for S^g which can be used as a probe for the estimation of the free carrier density in doped tubes. According to this expression S^g shows an activated T dependence at low temperatures. Screening effects of the carrier-phonon coupling reduce the magnitude of S^g severely and result to a quasilinear T dependence of phonon drag at high T. Finally, we have compared our model with available data in acid-doped bulk samples[8,9] and we found a very good agreement in a wide temperature range.

ACKNOWLEDGMENTS

The author wishes to thank K. Papagelis for extensive and useful discussions and R. Fletcher for stimulating remarks.

*rtsaous@upatras.gr

[1] L. Grigorian, K. A. Williams, S. Fang, G. U. Sumanasekera, A. L. Loper, E. C. Dickey, S. J. Pennycook, and P. C. Eklund, Phys. Rev. Lett. **80**, 5560 (1998); L. Grigorian, G. U. Sumanasekera, A. L. Loper, S. Fang, J. L. Allen, and P. C. Eklund, Phys. Rev. B **58**, R4195 (1998).
[2] J. Hone, I. Ellwood, M. Muno, A. Mizel, M. L. Cohen, A. Zettl, A. G. Rinzler, and R. E. Smalley, Phys. Rev. Lett. **80**, 1042 (1998).
[3] J. Hone, M. C. Llaguno, N. M. Nemes, A. T. Johnson, J. E. Fischer, D. A. Walters, M. J. Casavant, J. Schmidt, and R. E. Smalley, Appl. Phys. Lett. **77**, 666 (2000).
[4] P. G. Collins, K. Bradley, M. Ishigami, and A. Zettl, Science **287**, 1801 (2000).
[5] K. Bradley, S.-H. Jhi, P. G. Collins, J. Hone, M. L. Cohen, S. G. Louie, and A. Zettl, Phys. Rev. Lett. **85**, 4361 (2000).
[6] G. U. Sumanasekera, C. K. W. Adu, S. Fang, and P. C. Eklund, Phys. Rev. Lett. **85**, 1096 (2000).
[7] H. E. Romero, G. U. Sumanasekera, G. D. Mahan, and P. C. Eklund, Phys. Rev. B **65**, 205410 (2002).
[8] J. Vavro, M. C. Llaguno, J. E. Fischer, S. Ramesh, R. K. Saini, L. M. Ericson, V. A. Davis, R. H. Hauge, M. Pasquali, and R. E. Smalley, Phys. Rev. Lett. **90**, 065503 (2003).
[9] W. Zhou, J. Vavro, N. M. Nemes, J. E. Fischer, F. Borondics, K. Kamarás, and D. B. Tanner, Phys. Rev. B **71**, 205423 (2005).
[10] J. P. Small, K. M. Perez, and P. Kim, Phys. Rev. Lett. **91**, 256801 (2003).
[11] C. Yu, L. Shi, Z. Yao, D. Li, and A. Majumdar, Nano Lett. **5**, 1842 (2005).
[12] M. C. Llaguno, J. E. Fischer, A. T. Johnson, and J. Hone, Nano Lett. **4**, 45 (2004).
[13] V. W. Scarola and G. D. Mahan, Phys. Rev. B **66**, 205405 (2002).
[14] G. D. Mahan, Phys. Rev. B **69**, 125407 (2004).
[15] G. D. Mahan, in *Thermoelectrics Handbook: Macro to Nano*, edited by D. M. Rowe (CRC Press, USA, 2006), p. 17-1.
[16] M. Bailyn, Phys. Rev. **120**, 381 (1960); **157**, 480 (1967).
[17] C. Herring, Phys. Rev. **96**, 1163 (1954).
[18] B. L. Gallagher and P. N. Butcher, in *Handbook on Semiconductors*, Vol. 1, edited by T. S. Moss and P. T. Landsberg (Elsevier, Amsterdam, 1992), p. 817.
[19] R. Fletcher, E. Zaremba, and U. Zeitler, in *Electron-Phonon Interactions in Low Dimensional Structures*, edited by L. Challis (Oxford Science, Oxford, 2003), p. 149.
[20] M. Tsaousidou, in *The Oxford Handbook in Nanoscience and Technology*, edited by A. V. Narlikar and Y. Y. Fu (Oxford University Press, Oxford, 2010), Vol. II, p. 477.
[21] M. A. Kuroda and J.-P. Leburton, Phys. Rev. Lett. **101**, 256805 (2008).
[22] H. Suzuura and T. Ando, Phys. Rev. B **65**, 235412 (2002).
[23] J.-C. Charlier, X. Blase, and S. Roche, Rev. Mod. Phys. **79**, 677 (2007).
[24] D. G. Cantrell and P. N. Butcher, J. Phys. C **20**, 1985 (1987); **20**, 1993 (1987).
[25] S. S. Kubakaddi and P. N. Butcher, J. Phys.: Condens. Matter **1**, 3939 (1989).
[26] S. M. Puri, Phys. Rev. **139**, A995 (1965).
[27] J. P. Jay-Gerin, Phys. Rev. B **12**, 1418 (1975).
[28] S. S. Kubakaddi, P. N. Butcher, and B. G. Mulimani, Phys. Rev. B **40**, 1377 (1989).
[29] S. K. Lyo, Phys. Rev. B **40**, 6458 (1989).
[30] T. M. Fromhold, P. N. Butcher, G. Qin, B. G. Mulimani, J. P. Oxley, and B. L. Gallagher, Phys. Rev. B **48**, 5326 (1993).
[31] M. Tsaousidou and P. N. Butcher, Phys. Rev. B **56**, R10044 (1997).
[32] M. F. Lin and Kenneth W.-K. Shung, Phys. Rev. B **47**, 6617 (1993).
[33] R. A. Jishi, M. S. Dresselhaus, and G. Dresselhaus, Phys. Rev. B **48**, 11385 (1993).
[34] L. M. Woods and G. D. Mahan, Phys. Rev. B **61**, 10651 (2000).
[35] G. D. Mahan, Phys. Rev. B **68**, 125409 (2003).
[36] J. Jiang, R. Saito, Ge. G. Samsonidze, S. G. Chou, A. Jorio, G.

Dresselhaus, and M. S. Dresselhaus, Phys. Rev. B **72**, 235408 (2005).
[37] V. N. Popov and P. Lambin, Phys. Rev. B **74**, 075415 (2006).
[38] A. De Martino and R. Egger, Phys. Rev. B **67**, 235418 (2003).
[39] G. Pennington, N. Goldsman, A. Akturk, and A. E. Wickenden, Appl. Phys. Lett. **90**, 062110 (2007).
[40] T. Ragab and C. Basaran, J. Appl. Phys. **106**, 063705 (2009).
[41] A. De Martino, R. Egger, and A. O. Gogolin, Phys. Rev. B **79**, 205408 (2009).
[42] B. K. Ridley, *Quantum Processes in Semiconductors* (Clarendon Press, Oxford, 1988).
[43] G. Fishman, Phys. Rev. B **34**, 2394 (1986).
[44] P. F. Maldague, Surf. Sci. **73**, 296 (1978).
[45] M. Tsaousidou, P. N. Butcher, and G. P. Triberis, Phys. Rev. B **64**, 165304 (2001).
[46] S. Das Sarma and V. B. Campos, Phys. Rev. B **47**, 3728 (1993).
[47] S. K. Lyo and D. Huang, Phys. Rev. B **66**, 155307 (2002).
[48] A. Raichura, M. Dutta, and M. A. Stroscio, J. Appl. Phys. **94**, 4060 (2003).
[49] G. Pennington and N. Goldsman, Phys. Rev. B **71**, 205318 (2005).
[50] A. Thess, R. Lee, P. Nikolaev, H. Dai, P. Petit, J. Robert, C. Xu, Y. H. Lee, S. G. Kim, A. G. Rinzler, D. T. Colbert, G. E. Scuseria, D. Tomanek, J. E. Fischer, and R. E. Smalley, Science **273**, 483 (1996).
[51] V. V. Afonin, Y. M. Galperin, and V. L. Gurevich, Zh. Eksp. Teor. Fiz. **87**, 335 (1984) [Sov. Phys. JETP **60**, 194 (1984)]; M. J. Kearney and P. N. Butcher, J. Phys. C **21**, L265 (1988); C. Castellani, C. Di Castro, M. Grilli, and G. Strinati, Phys. Rev. B **37**, 6663 (1988).
[52] P. A. Lee and T. V. Ramakrishnan, Rev. Mod. Phys. **57**, 287 (1985).
[53] H. R. Shea, R. Martel, and Ph. Avouris, Phys. Rev. Lett. **84**, 4441 (2000).
[54] J. Vavro, J. M. Kikkawa, and J. E. Fischer, Phys. Rev. B **71**, 155410 (2005).
[55] L. Langer, V. Bayot, E. Grivei, J.-P. Issi, J. P. Heremans, C. H. Olk, L. Stockman, C. Van Haesendonck, and Y. Bruynseraede, Phys. Rev. Lett. **76**, 479 (1996).
[56] A. Miele, R. Fletcher, E. Zaremba, Y. Feng, C. T. Foxon, and J. J. Harris, Phys. Rev. B **58**, 13181 (1998); C. Rafael, R. Fletcher, P. T. Coleridge, Y. Feng, and Z. R. Wasilewski, Semicond. Sci. Technol. **19**, 1291 (2004).
[57] W. Zhou, J. Vavro, C. Guthy, K. I. Winey, J. E. Fischer, L. M. Ericson, S. Ramesh, R. Saini, V. A. Davis, C. Kittrell, M. Pasquali, R. H. Hauge, and R. E. Smalley, J. Appl. Phys. **95**, 649 (2004).